Hindawi
Wireless Communications and Mobile Computing
Volume 2018, Article ID 4765425, 7 pages
https://doi.org/10.1155/2018/4765425

Research Article

Magnetoelectric Dipole Antenna with Dual Polarization and High Isolation

Xujun Yang,[1] Lei Ge,[1] Dengguo Zhang,[1] and Chow-Yen-Desmond Sim[2]

[1]*College of Electronic Science and Technology, Shenzhen University, Shenzhen, China*
[2]*Department of Electrical Engineering, Feng Chia University, Taichung, Taiwan*

Correspondence should be addressed to Lei Ge; leige@szu.edu.cn

Received 5 December 2017; Accepted 28 February 2018; Published 11 April 2018

Academic Editor: Eva Antonino-Daviu

A dual-polarized aperture-coupled magnetoelectric (ME) dipole antenna is presented in this paper. The feeding network is based on substrate-integrated coaxial lines (SICLs). To describe the effect of the SICL on improving the isolation, the ME dipole with another two different feeding configurations, microstrip lines and striplines, respectively, is compared. As such, the coupling between the transmission lines is tremendously reduced and the isolation between the two input ports of different polarization is enhanced. An antenna prototype is fabricated and tested, exhibiting good performances, including an isolation level of higher than 30 dB between the two input ports and gains of more than 9.5 dBi. Besides, the proposed design is capable of achieving stable directional radiation patterns with cross-polarization levels lower than −22 dB and back radiation levels lower than −24 dB.

1. Introduction

Since the 5G (fifth-generation) wireless communication technology will be commercially available in the early 2020s, the number of mobile subscribers will rise enormously and mobile wireless services will unceasingly expand. Due to limited frequency resources, antennas with higher performances are desired to enhance the traffic capacity and spectrum utilization for wireless cellular networks.

Dual-polarized antennas are widely used in radio frequency communication systems, especially in mobile cellular base stations. Compared to linearly polarized antennas, dual-polarized antennas are more attractive because they can combat the multipath fading and increase the channel capacity [1]. Up to now, in order to obtain stable electrical performances, several dual-polarized antenna designs have been reported [2–4] on the basis of a wideband complementary antenna, namely, magnetoelectric (ME) dipole [5, 6]. This type of antenna comprises a vertically oriented quarter-wavelength shorted patch and a planar dipole, which behave as a magnetic dipole and an electric dipole. By exciting both the magnetic and electric dipoles with equal amplitudes and phases simultaneously, the antenna can achieve excellent performances, such as a wide impedance bandwidth, a stable gain, low back radiation, low cross-polarization levels, and symmetric E-plane and H-plane radiation patterns across the operating frequency band. Moreover, due to the aforementioned advantages, the ME dipole antenna can also be developed in the millimeter-wave band [7].

In this paper, we demonstrate a dual-polarized aperture-coupled ME dipole antenna. Its feeding network is based on substrate-integrated coaxial lines (SICLs), which is able to reduce the coupling between the transmission lines and therefore enhance the isolation between the two input ports of different polarization. In addition, a two-way power divider is used to realize a twin feed for balanced excitation. This leads to the proposed design with symmetric radiation patterns over its entire operating frequency band. Furthermore, nearly identical impedance matching and radiation performances are obtained for the two polarization levels.

2. Antenna Configuration

The geometry of the proposed dual-polarized aperture-coupled ME dipole antenna is given in Figure 1. Its detailed geometry dimensions are shown in Table 1. The antenna consists of three parts, including an ME dipole, a feeding

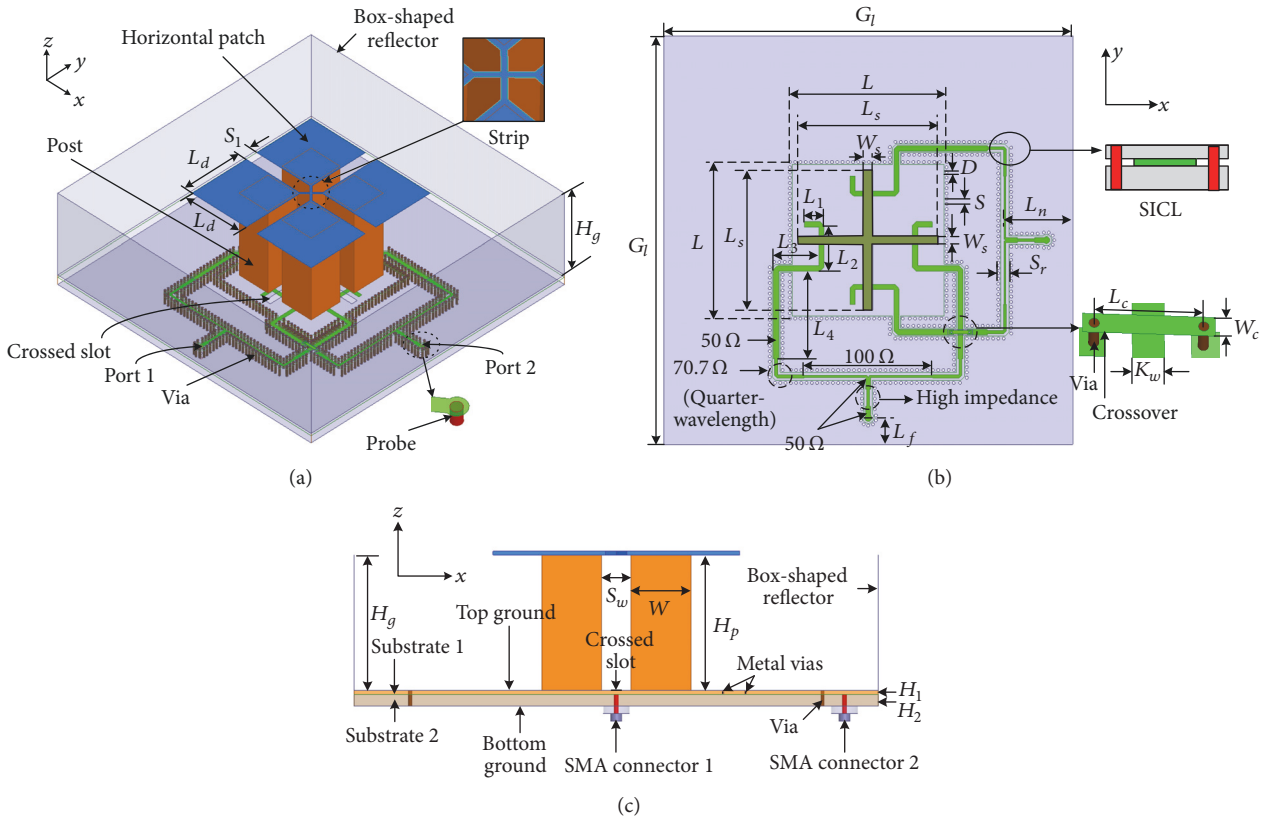

FIGURE 1: Geometry of the proposed dual-polarized aperture-coupled magnetoelectric dipole antenna. (a) 3D view. (b) Top view. (c) Side view.

network, and a box-shaped reflector. As shown in Figure 1(a), the ME dipole is composed of four parts which are located symmetrically with respect to the center of the ground plane. The four horizontal patches of the ME dipole are connected by a cross-shaped strip in the perpendicularly diagonal directions for impedance matching as analyzed in [7]. The ME dipole is aperture-coupled fed by a crossed slot. The structure of the feeding network is fabricated on two stacked substrates, namely, *Substrate 1* (Taconic RF-30, height of $H_1 = 1$ mm, $\varepsilon_r = 3$) and *Substrate 2* (Taconic TLC, height of $H_2 = 3.18$ mm, $\varepsilon_r = 3.2$). As illustrated in Figure 1(b), a two-way power divider is used to realize a twin feed for balanced excitation of the crossed slot. In order to locate the feeding network of the two polarization levels, a crossover is built in *Substrate 1*. As such, the ME dipole can be excited by the crossed slot. In this configuration, *Substrate 1* is reallocated on the top of *Substrate 2*, as shown in Figure 1(c). Lastly, a box-shaped reflector is employed to achieve stable radiation patterns and reduce the back lobe.

In this design, the SICL is realized by loading shorting vias with a periodic spacing along a stripline that is used to form the feeding network, and a backed cavity is also used (for the crossed slot) to suppress the back radiation of the ME dipole.

Here, *Substrate 2* (with a higher profile) is located below *Substrate 1* (with a lower profile), and they are firmly stacked together by applying several plastic screws. By doing so, the current distribution on the top ground of the two stacked substrates can be concentrated, which in this case will strengthen the excitation field around the cross slot loaded on the top ground [8].

3. Simulated and Measured Results

To verify the proposed design, a prototype was fabricated and tested. Simulated results were achieved by using the commercial EM software Ansys HFSS, including reflection coefficients ($S11$ and $S22$), isolation ($|S12|$), antenna gains, and radiation patterns. Measured results were obtained by using Agilent N5225A network analyzer and a Satimo Starlab near-field measurement system.

Figures 2(a) and 2(b) present the simulated and measured reflection coefficients of the proposed antenna at Port 1 and Port 2, respectively. Here, it can be seen that two resonances are excited, and the corresponding simulated impedance bandwidths (VSWR ≤ 1.5) via both ports ($S11$ and $S22$) are identical to each other at 23.4% (2.11–2.67 GHz), because of the symmetric structure of the proposed antenna. As for the measured reflection coefficients of the proposed antenna, Figures 2(a) and 2(b) show that the two resonances are slightly shifted to the higher frequency band. Notably, the differences between the measured and simulated reflection coefficients of the proposed antenna via both ports can be due to the

Table 1: Dimensions of the proposed antenna.

Parameters	G_l	L	L_S	L_d	W_S	H_P	W	H_g	S_W	S_I	D	S	S_r	L_n	L_C	L_f	K_W	W_C	L_1	L_2	L_3	L_4
Values/mm	140	52	48	30	1.5	36	16	36	7.8	5.8	1	1.8	4.4	23.3	6.1	9.1	1.8	1.2	6.8	15	15.5	30.2

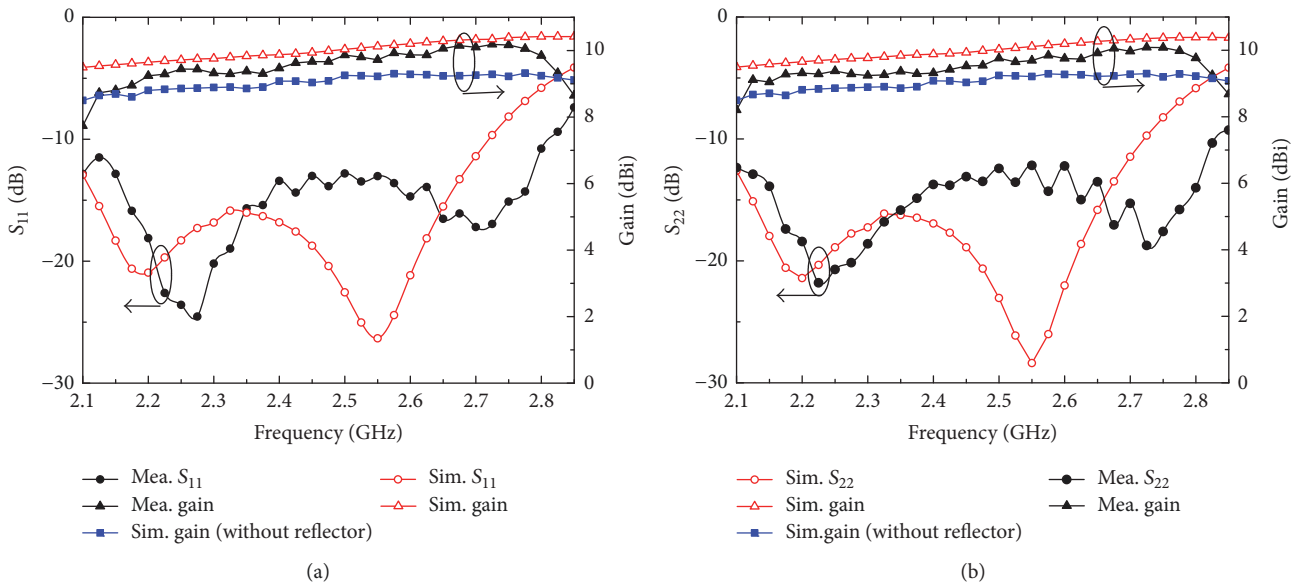

FIGURE 2: Simulated and measured reflection coefficients and broadside gains of the proposed antenna: (a) Port 1; (b) Port 2.

inevitable variations (because of fabrication inaccuracy) that exist between the exact dimensions of the fabricated prototype and the simulated one. Other effects such as imperfect SMA connector assembly and unavoidable small air gap between the two substrate layers may have also contributed to the differences.

The simulated and measured broadside gains of Ports 1 and 2 are also plotted in Figure 2. Within the operating frequency band, the measured gains are approximately 9.4 dBi with a variation of 0.6 dBi, which agrees well with the simulated result of 10 dBi with a variation of 0.5 dBi. Meanwhile, to evaluate how well the box-shaped reflector can increase the gains of both ports, the gain curves without reflector are presented for comparison. As observed from Figure 2, approximately 1.2 dBi of the increments is obtained at two ports. Figure 3 depicts the simulated and measured isolation between Ports 1 and 2. Over the operating frequency band, the simulated and measured results are very consistent with an isolation level of higher than 30 dB. Figure 3 also illustrates the measured antenna efficiencies of the proposed antenna. In the whole operating frequency band, the measured antenna efficiency is always larger than 83%.

The *E*-plane (*xoz*-plane) and *H*-plane (*yoz*-plane) radiation patterns of Port 1 at frequencies of 2.2, 2.4, and 2.6 GHz were illustrated in Figure 4. The radiation patterns of Port 2 are similar to that of Port 1 and are not given here for brevity. It can be observed that a good agreement between the measurement and the simulation is obtained. Across the operating frequency band, the proposed antenna is capable of realizing stable directional radiation patterns with cross-polarization levels lower than −22 dB and back radiation levels lower than −24 dB for both ports. The slight difference between the measured and simulated radiation patterns is mainly caused by fabrication inaccuracy and manufacturing soldering tolerances.

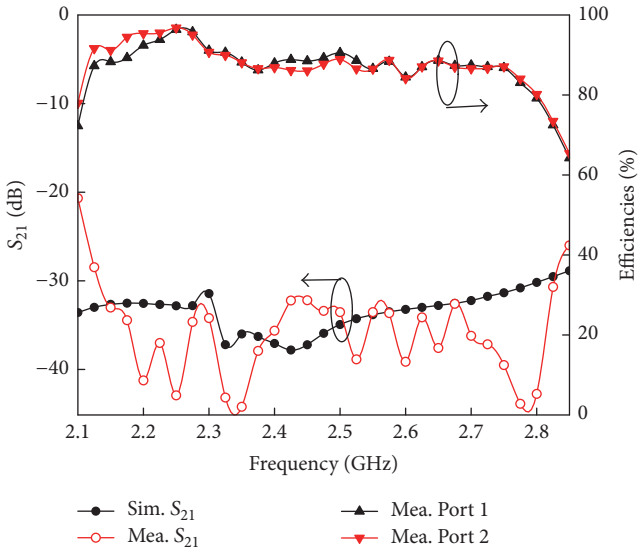

FIGURE 3: Simulated and measured S_{21} and efficiencies of the proposed antenna.

4. Comparison and Discussion

4.1. Feeding Configurations. For a dual-polarized antenna, the isolation between the two polarization levels is one of the most significant characteristics. To show how well the SICL feeding network can improve the isolation of the proposed ME dipole antenna, two different (typically used) feeding configurations are also investigated via simulation. Figures 5 and 6 show the impedance matching and isolation of the proposed ME dipole antenna when applying the microstrip lines and striplines as transmission lines of the feeding network, respectively.

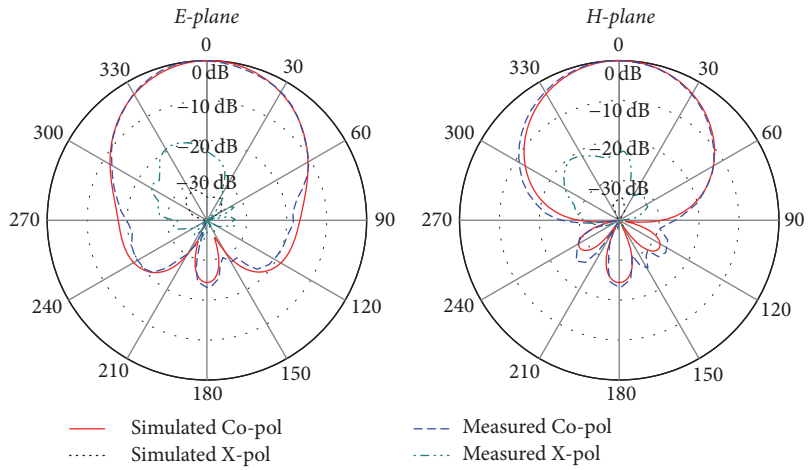

(a)

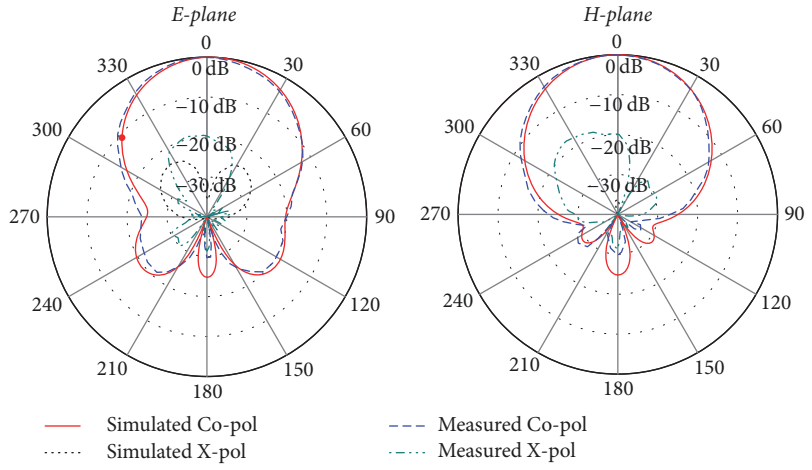

(b)

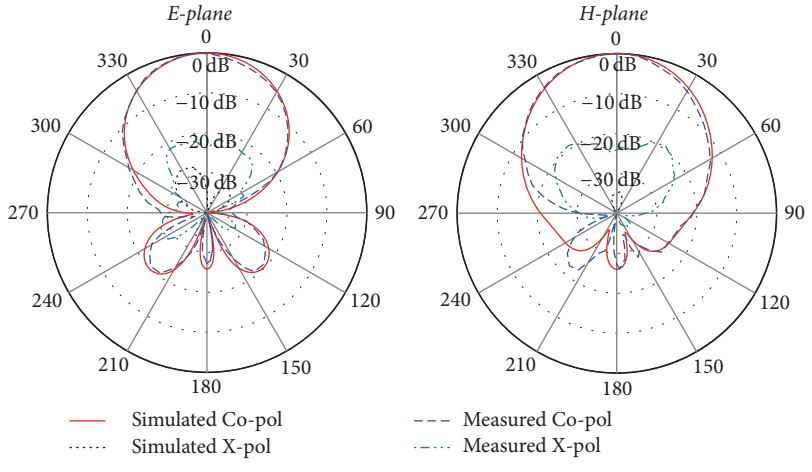

(c)

Figure 4: Simulated and measured radiation patterns of E-plane and H-plane at Port 1. (a) 2.2 GHz; (b) 2.4 GHz; (c) 2.6 GHz.

As shown in Figure 5, the two resonances are separated farther away from each other, leading to two operating modes with narrow 10-dB impedance bandwidths at approximately 2.1 and 2.7 GHz. By further observing S_{21} across the operating frequency, isolation level of up to 23 dB is observed. As shown in Figure 6, much poorer impedance matching is observed across the operating frequency when the SICLs are replaced by the striplines. As for its corresponding S_{21}, undesirable

Table 2: Comparison between proposed and reported dual-polarized ME dipole antennas.

Ref.	Antenna size (λ_0^3)	Impedance bandwidth %	Average gain (dBi)	Isolation (dB)
[2]	1.28 ∗ 1.28 ∗ 0.23	65.9 (SWR < 2)	9.5	36
[3]	0.82 ∗ 0.82 ∗ 0.15	25.2 and 32.2 (SWR < 2)	8.2	29
[4]	1.3 ∗ 1.3 ∗ 0.24	68 (SWR < 2)	8.1	36
This work	1.12 ∗ 1.12 ∗ 0.32	23.4 (SWR < 1.5)	9.5	30

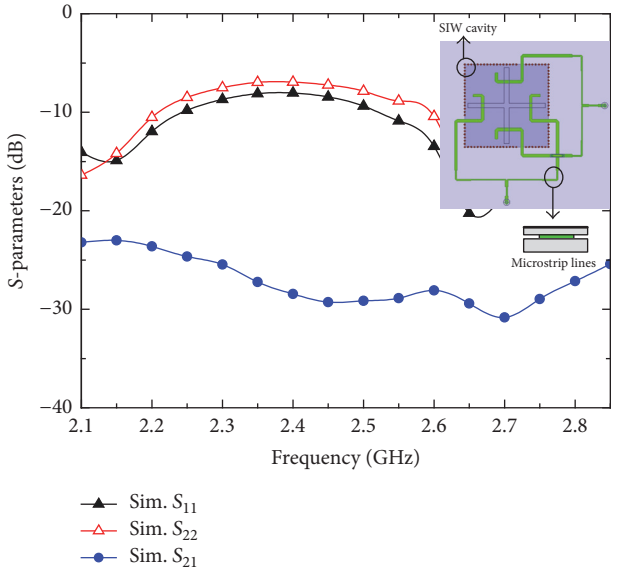

Figure 5: Proposed ME dipole antenna fed by microstrip lines.

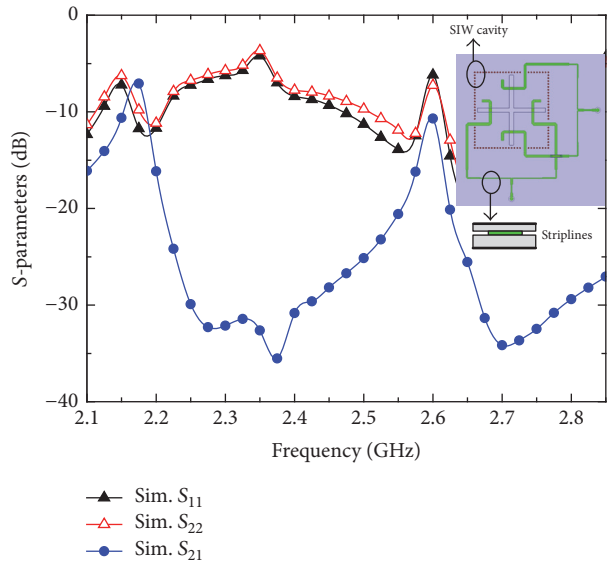

Figure 6: Proposed ME dipole antenna fed by striplines.

isolation of approximately 7 dB and 11 dB is realized at 2.18 GHz and 2.59 GHz, respectively. Here, it is worth noting that because of the change in characteristic impedance of the transmission lines, even though the impedances of the above two different feeding configurations are not well matched, the isolation levels can still be used as a reference, because the isolation levels of the above two investigated cases will be even lower when the proposed antenna is impedance matched. Therefore, if the above two investigated cases have been modified to attain good impedance matching, the isolation of the microstrip lines case will not be better than 23 dB, and the isolation level of the striplines case will be even worse than 9 dB (at 2.16 GHz). For comparison, the isolation level is higher than 30 dB over the entire operating band when SICLs are applied to the proposed antenna. This is because the electromagnetic field is well sealed in the SICLs; therefore, the coupling between adjacent transmission lines is weak. Lastly, the photograph of the fabricated prototype is presented in Figure 7.

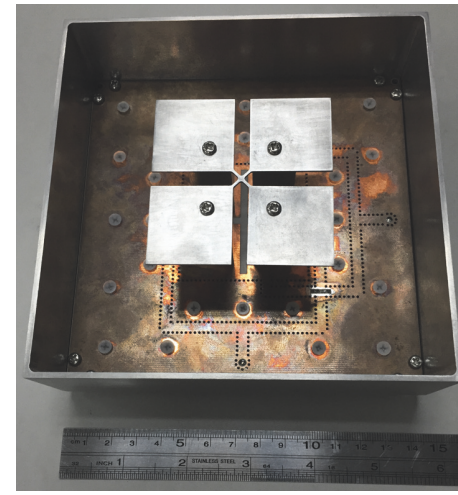

Figure 7: Prototype of the fabricated antenna.

4.2. Performances. Table 2 compares the proposed ME dipole antenna's performances with other published dual-polarized ME dipole antennas. In terms of the bandwidth and isolation, although [2, 4] can achieve more than 60% impedance bandwidths and larger than 36 dB isolation, their horizontal geometry dimensions are slightly wider. Especially in [4], a higher isolation is realized by differential feeding, and thus the complexity will be raised inevitably. The design in [3] can reduce the size of the antenna with dielectric loading but suffer from asymmetrical impedance bandwidths and lower gains between the two ports. By comparison, this work still has significant value with a stable gain of 9.5 dBi and high isolation and wide bandwidths via both ports.

5. Conclusion

A dual-polarized aperture-coupled ME dipole antenna with feeding network that is based on the SICL has been successfully investigated. To validate the performances of the design, an elevated prototype was fabricated and measured. The measured results show that the proposed ME dipole antenna has wide bandwidths, stable gains, well-controlled radiation patterns, and high isolation between different polarization levels.

Conflicts of Interest

The authors declare that they have no conflicts of interest.

References

[1] S. Gao, A. Sambell, and S. S. Zhong, "Polarization-agile antennas," *IEEE Antennas and Propagation Magazine*, vol. 48, no. 3, pp. 28–37, 2006.

[2] B. Q. Wu and K. M. Luk, "A broadband dual-polarized magneto-electric dipole antenna with simple feeds," *IEEE Antennas and Wireless Propagation Letters*, vol. 8, pp. 60–63, 2009.

[3] L. Siu, H. Wong, and K. M. Luk, "A dual-polarized magneto-electric dipole with dielectric loading," *IEEE Transactions on Antennas and Propagation*, vol. 57, no. 3, pp. 616–623, 2009.

[4] Q. Xue, S. W. Liao, and J. H. Xu, "A differentially-driven dual-polarized magneto-electric dipole antenna," *IEEE Transactions on Antennas and Propagation*, vol. 61, no. 1, pp. 425–430, 2013.

[5] K. M. Luk and H. Wong, *A complementary wideband antenna*, U.S. Patent No. 11/373,518, Mar. 10, 2006.

[6] K. M. Luk and H. Wong, "A new wideband unidirectional antenna element," *Int. J. Microw. Opt. Technol*, vol. 1, no. 1, pp. 35–44, 2006.

[7] Y. Li and K. M. Luk, "60-GHz Dual-Polarized Two-Dimensional Switch-Beam Wideband Antenna Array of Aperture-Coupled Magneto-Electric Dipoles," *IEEE Transactions on Antennas and Propagation*, vol. 64, no. 2, pp. 554–563, 2016.

[8] P. Brachat and J. M. Baracco, "Dual-Polarization Slot-Coupled Printed Antennas Fed by Stripline," *IEEE Transactions on Antennas and Propagation*, vol. 43, no. 7, pp. 738–742, 1995.